

Achievable Information Rates and Concatenated Codes for the DNA Nanopore Sequencing Channel

Issam Maarouf*, Eirik Rosnes*, and Alexandre Graell i Amat†

*Simula UiB, N-5006 Bergen, Norway

†Department of Electrical Engineering, Chalmers University of Technology, SE-41296 Gothenburg, Sweden

Abstract—The errors occurring in DNA-based storage are correlated in nature, which is a direct consequence of the synthesis and sequencing processes. In this paper, we consider the memory- k nanopore channel model recently introduced by Hamoum *et al.*, which models the inherent memory of the channel. We derive the maximum a posteriori (MAP) decoder for this channel model. The derived MAP decoder allows us to compute achievable information rates for the true DNA storage channel assuming a mismatched decoder matched to the memory- k nanopore channel model, and quantify the loss in performance assuming a small memory length—and hence limited decoding complexity. Furthermore, the derived MAP decoder can be used to design error-correcting codes tailored to the DNA storage channel. We show that a concatenated coding scheme with an outer low-density parity-check code and an inner convolutional code yields excellent performance.

I. INTRODUCTION

Storing data in deoxyribonucleic acid (DNA) promises unprecedented density and durability and is seen as the new frontier of data storage. Recent experiments have already demonstrated the viability of DNA-based data storage [1]–[3].

The DNA storage channel suffers from multiple impairments and constraints due to the synthesis and sequencing of DNA and the limitations of current technologies. In particular, errors in the form of insertions, deletions, and substitutions (IDS) occur. This has spurred a great deal of research on devising coding schemes for the DNA storage channel.

While the literature on error-correcting coding for the DNA storage channel is abundant, most works have considered a simplified and unrealistic channel model with a small and fixed number of insertions and/or deletions, i.e., an *adversarial* channel. Fewer works have considered a more realistic probabilistic channel model in which errors occur with a given probability, e.g., [4]–[16]. These works usually assume independent and identically distributed (i.i.d.) errors. In DNA storage, however, IDS errors are not i.i.d., but the channel has memory [17], [18]. Potentially, the memory is as large as the whole DNA sequence.

In [17], the authors proposed a statistical model of the DNA storage channel with nanopore sequencing based on a Markov chain that models the inherent memory of the channel. In particular, it builds on the fact that in the MinION technology strands traverse a nanopore nucleotide by nucleotide, and an

electrical signal is generated for every group of $k \geq 1$ successive nucleotides, called k mers. Let x be the DNA strand to be synthesized and z be the sequence of channel events, where $z_i \in \{\text{insertion, deletion, substitution, no error}\}$. The key idea in [17] is then to assume that z_i depends on the symbols x_{i-k+1}, \dots, x_i and the previous event z_{i-1} and estimate the probabilities $p(z_i | x_{i-k+1}, \dots, x_i, z_{i-1})$ from experimental data. We refer to this channel model as the memory- k nanopore channel model.

The starting point of this paper is the work [17]. Our main contributions are as follows.

- We derive the optimum maximum a posteriori (MAP) decoder for the memory- k nanopore channel model. The complexity of the decoder increases exponentially with k . Based on this decoder, we derive achievable information rates (AIRs).
- The AIR for the memory- k nanopore channel can be seen as an AIR for the true DNA storage channel of a *mismatched* decoder (i.e., a decoder that is not matched to the true channel) that assumes that the channel is a memory- k nanopore channel. We show that for increasing k , the AIR improves—meaning that the decoder is better matched to the true channel—and eventually saturates. This allows us to quantify the trade-off between decoding complexity and performance loss incurred by the suboptimal decoder.
- The derived MAP decoder can be used to design error-correcting coding schemes tailored to the memory- k nanopore sequencing channel. In particular, we consider the concatenated coding scheme proposed in [4] and multiple reads of the DNA strand, and we optimize the inner and outer code. We show that the concatenated coding scheme of [4] yields excellent performance at rates close to the AIRs.
- We validate the AIRs and simulation results of the memory- k nanopore channel model using the dataset of DNA reads in [6] obtained using Oxford Nanopore Technologies (ONT) sequencing with the MinION technology.

II. THE NANOPORE SEQUENCING CHANNEL MODEL

We consider the memory- k nanopore channel model introduced in [17]. The key property of this channel model is that it removes the assumption of i.i.d. IDS errors. In particular, the occurrence of an error event, or a correct transmission, depends on the previous event (an insertion, deletion, substitution, or

The work of A. Graell i Amat was supported by the Swedish Research Council under grant 2020-03687.

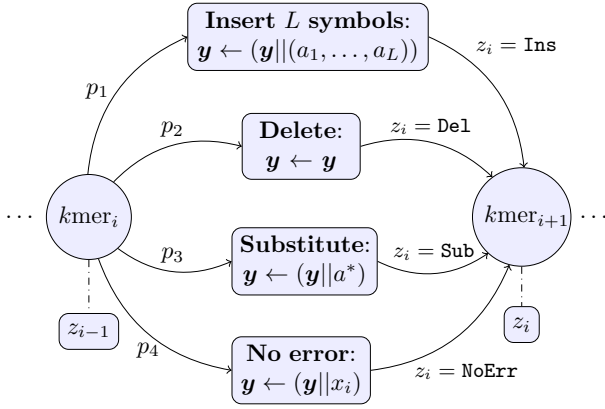


Fig. 1. The memory- k nanopore channel in [17].

no error event), and previous channel input symbols. Let $\mathbf{x} = (x_1, \dots, x_N)$, $x_i \in \Sigma_4 = \{0, 1, 2, 3\}$, be the channel input sequence and $\mathbf{y} = (y_1, \dots, y_{N'})$ the channel output sequence, and define $x_{N+1} = 0$. Note that N' is random and depends on the number of insertion and deletion events, i.e., $N' \neq N$ in general. Also, let $kmer_i = (x_{i-k+1}, \dots, x_i)$ be the $kmer$ at time instant $i \geq k$, while for $i < k$, since no complete $kmer$ is available, we use $kmer_i = x_i$. The channel model is depicted in Fig. 1. Here, we denote the event associated with $kmer_{i+1}$ by z_i , where z_i represents an insertion, deletion, substitution, or no error acting on symbol x_i when it is to be transmitted. Hence, $z_i \in \{\text{Ins}, \text{Del}, \text{Sub}, \text{NoErr}\}$. The transition probabilities p_1 , p_2 , p_3 , and p_4 in the figure are of the form $p(z_i | kmer_i, z_{i-1})$, and their value depends on the $kmer$. In the event of a deletion, the symbol x_i in $kmer_i$ will be deleted and nothing will be appended to \mathbf{y} , while when a no error event occurs, \mathbf{y} will be appended with x_i . Furthermore, in the event of an insertion, i.e., $z_i = \text{Ins}$, the channel will insert $L > 1$ symbols a_1, \dots, a_L , where the length L is random. Each symbol a_j will be uniformly picked from Σ_4 . In this case, the channel appends \mathbf{y} with (a_1, \dots, a_L) . This also applies to a substitution event where the symbol a^* is uniformly picked from $\Sigma_4 \setminus \{x_i\}$ and appended to \mathbf{y} instead of x_i . Moreover, we define $p(L | kmer_i, z_i = \text{Ins})$ as the probability of inserting L symbols given $kmer_i$ and an insertion event, and $p(a^* | kmer_i, z_i = \text{Sub})$ as the probability of x_i being substituted by a^* given $kmer_i$ and a substitution event. In all these scenarios, the channel always moves from state $kmer_i$ to state $kmer_{i+1}$. After the last symbol x_N has been processed by the channel, the channel outputs \mathbf{y} .

A. Channel Transition Probability Estimation

The transition probabilities of the channel model can be estimated using a DNA storage dataset \mathcal{D} containing input (before synthesis) and the corresponding multiple output (after sequencing) sequences.

Let $\mathbf{x}^{(l)}$ denote the l -th input sequence and $\mathbf{y}_1^{(l)}, \dots, \mathbf{y}_{M_l}^{(l)}$ the corresponding $M_l \geq 1$ output sequences from the dataset \mathcal{D} . The method we use to estimate the transition probabilities is as follows. For each pair $(\mathbf{x}^{(l)}, \mathbf{y}_j^{(l)})$, we compute the edit distance between the two vectors using a lattice (see [4,

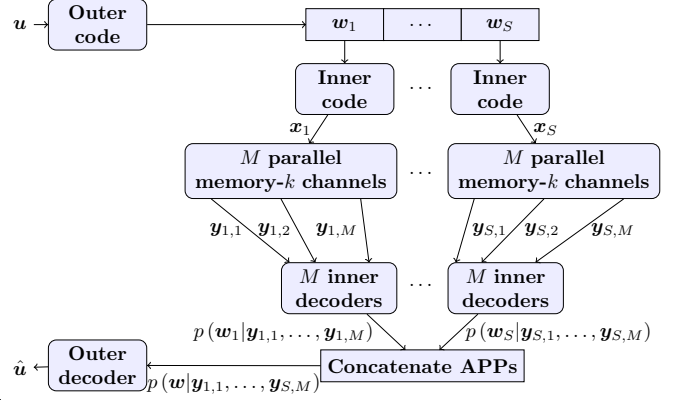


Fig. 2. System model including the coding scheme and the memory- k nanopore channel model depicted in Fig. 1.

Sec. III], [19]). By backtracking from the end of the lattice, a corresponding sequence of events $z_j^{(l)}$ can be identified. In case of ties, one event is chosen uniformly at random. Finally, we estimate the probabilities $p(z_i = z | kmer_i = kmer, z_{i-1} = z')$ by a simple counting argument. In particular, let

$$\mathcal{S}_{z, z', kmer}^{(l, j)} = \{k \leq u < N : (x_{u-k+1}^{(l)}, \dots, x_u^{(l)}) = kmer, (z_{j, u-1}^{(l)}, z_{j, u}^{(l)}) = (z', z)\}.$$

Then, for $k \leq i < N$, $p(z_i = z | kmer_i = kmer, z_{i-1} = z')$ is estimated by

$$\frac{\sum_{l=1}^{|\mathcal{D}|} \sum_{j=1}^{M_l} |\mathcal{S}_{z, z', kmer}^{(l, j)}|}{\sum_{z \in \{\text{Ins}, \text{Del}, \text{Sub}, \text{NoErr}\}} \sum_{l=1}^{|\mathcal{D}|} \sum_{j=1}^{M_l} |\mathcal{S}_{z, z', kmer}^{(l, j)}|}.$$

As a consequence, the channel parameters do not vary with i for $k \leq i < N$. For $1 < i < k$, we estimate the channel transition probabilities in a similar manner as above, but considering that $kmer_i = x_i$. Moreover, as in [17], we consider $i = 1$ (the beginning) and $i = N$ (the end) separately from the middle ($1 < i < N$) when estimating the channel parameters as the probability to get an error is typically higher at the beginning and at the end compared to the middle.

B. Multiple Reads

We consider the relevant scenario in which the sequencing process outputs multiple reads (M) of the DNA strand. In particular, we model this by assuming that a strand is transmitted over M independent channels.

III. CODING SCHEME AND SYSTEM MODEL

We consider the concatenated coding scheme and the low-complexity *separate decoding* scheme proposed in [4], which decodes separately each noisy strand and combines a posteriori probabilities (APPs) from all reads before passing them to the outer decoder. The primary goal of the inner code is to maintain synchronization with the transmitted sequence and provide likelihoods to the outer decoder. The outer code then corrects remaining errors.

The system model is shown in Fig. 2. We consider a low-density parity-check (LDPC) code for the outer code and a

convolutional code for the inner code. The information data $\mathbf{u} = (u_1, \dots, u_K)$, $u_i \in \mathbb{F}_{q_o}$, of length K , is first encoded by an $[N_o, K]_{q_o}$ outer LDPC code over \mathbb{F}_{q_o} into the codeword $\mathbf{w} = (w_1, \dots, w_{N_o})$, $w_i \in \mathbb{F}_{q_o}$, where \mathbb{F}_{q_o} is a binary extension field of size $2^{k_{cc}}$ and k_{cc} is the (binary) dimension of the inner convolutional code. Since current sequencing technologies cannot handle long sequences, the codeword \mathbf{w} is split into S subsequences $\mathbf{w}_1, \dots, \mathbf{w}_S$, each of length $N_o^b = N_o/S$, where $\mathbf{w}_j = (w_{(j-1)N_o^b+1}, \dots, w_{jN_o^b})$. Each \mathbf{w}_j is encoded, with an optional offset [4], by an $(n, k_{cc}, m)_4$ inner convolutional code of binary dimension k_{cc} , memory m , and output alphabet Σ_4 into the inner codeword \mathbf{x}_j of length $N = (N_o^b + m)n$, where m is due to terminating the convolutional code to the all-zero state. The overall code rate is given as $R = R_o R_i = K_{k_{cc}}/S N$, where $R_o = K/N_o$ is the rate of the outer code and $R_i = k_{cc} N_o^b/N$ the rate of the inner code.

Each \mathbf{x}_j is transmitted independently over M identical memory- k nanopore channels in order to model the multiple copies of a DNA strand at the output of the sequencing process. At the receiver, each noisy read $\mathbf{y}_{j,1}, \dots, \mathbf{y}_{j,M}$ for transmitted sequence \mathbf{x}_j is decoded separately with a MAP inner decoder. The APPs at their output are then combined to provide approximate APPs for w_j . The (approximate) APPs for the symbols in $\mathbf{w} = (\mathbf{w}_1, \dots, \mathbf{w}_S)$ are concatenated and then passed to the outer decoder. The outer decoder uses these APPs to decide on an estimate $\hat{\mathbf{u}}$ of \mathbf{u} .

IV. SYMBOLWISE MAP DECODING FOR CHANNEL/INNER CODE (INNER DECODING)

In this section, we derive the optimum (MAP) decoder for the combination of the memory- k nanopore channel model and the inner code. To this end, we use the fact that the combination of the channel and the inner code can be seen as a hidden Markov model (HMM) by introducing a *drift* variable as in [7]. The drift d_i , $0 \leq i < N_o^b + m$, is defined as the number of insertions minus the number of deletions that occurred before symbol x_{ni+1} is to be acted on by the event z_{ni+1} , while $d_{N_o^b+m}$ is defined as the number of insertions minus deletions that occurred after the last symbol x_N has been processed by the channel. Thus, by definition, $d_0 = 0$ and $d_{N_o^b+m} = N' - N$, both known to the decoder. Adding the drift to the joint state of the channel and the inner code, i.e., to $(kmer_{i+1}, z_i, s_i)$, where s_i denotes the state variables of the inner convolutional code, gives the state variable $\sigma_i = (kmer_{i+1}, z_i, s_i, d_i)$ of the HMM. In this HMM, a transition from time $i-1$ to time i corresponds to a transmission of symbols $\mathbf{x}_{(i-1)n+1}^{in}$, where $\mathbf{x}_a^b = (x_a, x_{a+1}, \dots, x_b)$. Further, when transitioning from a state with drift d_{i-1} to a state with drift d_i , the HMM emits $n + d_i - d_{i-1}$ output symbols depending on both the previous and new drift.

In the following, to simplify notation, the subsequence index of \mathbf{w} and \mathbf{y} is omitted and w_i simply refers to the i -th symbol of an arbitrary subsequence \mathbf{w}_j , while $\mathbf{y} = (\mathbf{y}_1, \dots, \mathbf{y}_M)$ refers to the corresponding received sequences.

A. Decoding for a Single Received Sequence

The APP for outer code symbol w_i can be computed as $p(w_i|\mathbf{y}) = p(\mathbf{y}, w_i)/p(\mathbf{y})$, where the joint probability $p(\mathbf{y}, w_i)$ can be computed by marginalizing the trellis states, corresponding to the HMM, of the channel/inner code that correspond to symbol w_i . Then, we can write $p(\mathbf{y}, w_i) = \sum_{(\sigma, \sigma'): w_i} p(\mathbf{y}, \sigma, \sigma')$, where σ and σ' are realizations of the random variables σ_{i-1} and σ_i , respectively. Here, the summation is over all pairs of states that correspond to symbol w_i . We can use the Markov property to decompose the probability $p(\mathbf{y}, \sigma, \sigma')$ into three parts as

$$p(\mathbf{y}, \sigma, \sigma') = p(\mathbf{y}_1^{(i-1)n+d}, \sigma) p(\mathbf{y}_{(i-1)n+d+1}^{in+d}, \sigma' | \sigma) p(\mathbf{y}_{in+d+1}^{N'} | \sigma').$$

We abbreviate the first, second, and third term of the above equation with $\alpha_{i-1}(\sigma)$, $\gamma_i(\sigma, \sigma')$, and $\beta_i(\sigma')$, respectively. Then, the first and third term can be computed recursively as

$$\alpha_i(\sigma') = \sum_{\sigma} \alpha_{i-1}(\sigma) \gamma_i(\sigma, \sigma'), \beta_{i-1}(\sigma) = \sum_{\sigma'} \beta_i(\sigma') \gamma_i(\sigma, \sigma').$$

The term $\gamma_i(\sigma, \sigma')$ (the branch metric) can be decomposed as

$$\gamma_i(\sigma, \sigma') = p(w_i) p(z' | kmer, z) \cdot p(\mathbf{y}_{(i-1)n+d+1}^{in+d}, d' | d, s, s', z', z, kmer', kmer),$$

where $p(w_i)$ is the a priori probability of symbol w_i . For simplicity, define the state variable $\zeta_i = (kmer_{i+1}, z_i)$. To compute $p(\mathbf{y}_{(i-1)n+d+1}^{in+d}, d' | d, s, s', \zeta', \zeta)$, we need to consider each possible event for z' . For simplicity, we limit our derivation to $n = 1$. The case for general n follows in a straightforward manner.

1) $z' = \text{Ins}$. Then,

$$\begin{aligned} & p(\mathbf{y}_{(i-1)+d+1}^{i+d}, d' | d, s, s', \zeta', \zeta) \\ &= p(\mathbf{y}_{(i-1)+d+1}^{i+d}, L = d' - d | d, s, s', \zeta', \zeta) \\ & \cdot p(L = d' - d | d, s, s', \zeta', \zeta) \\ &= \left(\frac{1}{4}\right)^L \cdot p(L | kmer, z' = \text{Ins}). \end{aligned}$$

2) $z' = \text{Del}$. Then, $d' = d - 1$, which means that

$$p(\mathbf{y}_{(i-1)+d+1}^{i+d}, d' \neq d - 1 | d, s, s', \zeta', \zeta) = 0 \text{ and } p(\mathbf{y}_{(i-1)+d+1}^{i+d}, d' = d - 1 | d, s, s', \zeta', \zeta) = 1.$$

3) $z' = \text{Sub}$. Then, $d' = d$, which means that

$$p(\mathbf{y}_{(i-1)+d+1}^{i+d}, d' \neq d | d, s, s', \zeta', \zeta) = 0, \text{ and}$$

$$\begin{aligned} & p(\mathbf{y}_{(i-1)+d+1}^{i+d}, d' = d | d, s, s', \zeta', \zeta) \\ &= \begin{cases} p(\mathbf{y}_{i+d}^{i+d} | kmer, s, s', z' = \text{Sub}) & \text{if } \mathbf{y}_{i+d}^{i+d} \neq \mathbf{x}_{i+d}^{i+d} \\ 0 & \text{otherwise.} \end{cases} \end{aligned}$$

4) $z' = \text{NoErr}$. Then, $d' = d$, which means that

$$p(\mathbf{y}_{(i-1)+d+1}^{i+d}, d' \neq d | d, s, s', \zeta', \zeta) = 0, \text{ and}$$

$$\begin{aligned} & p(\mathbf{y}_{(i-1)+d+1}^{i+d}, d' = d | d, s, s', \zeta', \zeta) \\ &= \begin{cases} 1 & \mathbf{y}_{i+d}^{i+d} = \mathbf{x}_{i+d}^{i+d} \\ 0 & \text{otherwise.} \end{cases} \end{aligned}$$

B. Decoding for Multiple Received Sequences

We consider the separate decoding strategy for multiple received sequences $\mathbf{y}_1, \dots, \mathbf{y}_M$ proposed in [4]. Following [4], the APP $p(w_i|\mathbf{y}_1, \dots, \mathbf{y}_M)$ can be approximated as

$$p(w_i|\mathbf{y}_1, \dots, \mathbf{y}_M) \approx \frac{\prod_{j=1}^M p(w_i|\mathbf{y}_j)}{p(w_i)^{M-1}},$$

where $p(w_i|\mathbf{y}_j)$ is computed as outlined in Section IV-A. This decoder, although suboptimal, is efficient and practical for our scenario, as its complexity grows linearly with M [4].¹

C. Decoding Complexity

Since the overall decoding complexity is dominated by the combination of the inner code and the channel, we will disregard the complexity of the outer decoder in the complexity analysis. In order to limit the inner decoding complexity, we limit the drift d_i to a fixed interval $[d_{\min}, d_{\max}]$ and the number of insertions per symbol L to L_{\max} ; recall also that $L > 1$. For simplicity, we limit our derivation to $n = 1$. The complexity of the BCJR algorithm on the joint trellis of the inner code and the channel is directly proportional to the number of trellis edges at each trellis section, which is upper bounded by $2^{\nu+k_{\text{cc}}} 4^{k+1} \Delta(\delta+1)$, where $\Delta = d_{\max} - d_{\min} + 1$ is the number of drift states, $\delta = L_{\max} + 1$ is the number of possible drift transitions, and ν is the number of binary memory elements of the convolutional encoder. Hence, the complexity of decoding a single block is $(N_{\circ}^b + m) 2^{\nu+k_{\text{cc}}} 4^{k+1} \Delta(\delta+1)$, and the complexity of separate decoding (for all S blocks) becomes $S(N_{\circ}^b + m) 2^{\nu+k_{\text{cc}}} 4^{k+1} \Delta(\delta+1)M$. Note that the complexity increases exponentially with the channel memory k .

V. ACHIEVABLE INFORMATION RATES

The MAP decoder for the memory- k nanopore channel (including the inner code) derived in Section IV allows us to compute AIRs for this channel. In particular, we compute *BCJR-once* rates [20]–[22], defined as the symbolwise mutual information between the input of the channel and the log-likelihood ratios (LLRs) produced by a symbolwise MAP (i.e., optimum) detector. For a given inner code, the BCJR-once rate, denoted by $R_{\text{BCJR-once}}$, is a rate achievable by an outer code that does not exploit possible correlations between the LLRs and when no iterations between the inner and outer decoder are performed.

The BCJR-once rate under separate decoding can be estimated as

$$R_{\text{BCJR-once}} \approx R_i \log q_{\circ} + \frac{R_i}{N_{\circ}^b + m} \sum_{i=1}^{N_{\circ}^b + m} \log \frac{e^{L_i^{\text{BCJR-sep}}(w_i)}}{\sum_{a \in \mathbb{F}_{q_{\circ}}} e^{L_i^{\text{BCJR-sep}}(a)}}$$

by sampling an input sequence \mathbf{w} and corresponding output sequence $\mathbf{y} = (\mathbf{y}_1, \dots, \mathbf{y}_M)$ and computing the (mismatched) LLRs $L_i^{\text{BCJR-sep}}(a) = \sum_{j=1}^M \ln \frac{q(w_i=a|\mathbf{y}_j)}{q(w_i=0|\mathbf{y}_j)}$, $a \in \mathbb{F}_{q_{\circ}}$, where $q(w_i|\mathbf{y}_j)$ is a (mismatched) inner decoding metric.

¹Alternatively, one may decode all M reads jointly using a single inner decoder [4]. However, the complexity of this decoder grows exponentially with the number of sequences M , and becomes infeasible for $M > 2$.

TABLE I
OPTIMIZED PROTOGRAPHS FOUND BY DE FOR DIFFERENT M

M	$R = R_{\circ}R_i$	Protograph
1	$8/10 \cdot 3/2 = 6/5$	$\begin{pmatrix} 1 & 2 & 0 & 1 & 2 & 2 & 1 & 1 & 1 & 3 \\ 2 & 0 & 3 & 2 & 1 & 0 & 1 & 2 & 2 & 0 \end{pmatrix}$
2	$7/8 \cdot 3/2 = 21/16$	$(2 \ 2 \ 3 \ 3 \ 2 \ 3 \ 3 \ 3)$
5	$14/15 \cdot 3/2 = 7/5$	$(3 \ 2 \ 3 \ 3 \ 2 \ 2 \ 3 \ 3 \ 2 \ 2 \ 3 \ 3 \ 3 \ 2 \ 3)$

BCJR-once rates can also be computed for the true DNA storage channel using a dataset of DNA traces by averaging over pairs of input and output sequences. In this case, given an inner code and a decoder that assumes that the channel has memory k , the BCJR-once rate is an AIR for the DNA storage channel of a *mismatched* decoder where the inner decoder is matched to the memory- k nanopore channel model.

For both cases, we assume separate decoding and an inner MAP decoder matched to the memory- k nanopore channel model, i.e., using $q(w_i|\mathbf{y}_j) = p(w_i|\mathbf{y}_j)$ where $p(w_i|\mathbf{y}_j)$ is computed as described in Section IV-A.

VI. CONCATENATED CODING SCHEME DESIGN

A. Inner Code

For the inner code we use the $(1, 1, 2)_4$ convolutional code with generator polynomial $g = [5, 7]_{\text{OCT}}$ and punctured in order to have a higher rate. In particular, we use the puncturing matrix $\mathbf{P} = \begin{pmatrix} 1 & 0 & 1 \\ 1 & 1 & 0 \end{pmatrix}$, which gives an inner code rate of $R_i = 3/2$ (in bits per DNA symbol). Moreover, we add a pseudo-random sequence to the output of the inner code.

B. Outer Code

We consider a protograph-based binary LDPC code as the outer code, which we optimize (also in terms of code rate) via density evolution (DE) using the algorithm proposed in [20] for the memory-5 nanopore channel model for $M = 1, 2$, and 5. Moreover, we set $N = 110$ as the dataset in [6] contains input sequences with this length. The optimized protographs, when limiting the entries to at most 3, are shown in Table I. The outer LDPC codes are constructed by lifting the protographs using circulants that are optimized using the progressive edge-growth algorithm [23].

VII. NUMERICAL RESULTS AND DISCUSSION

In this section, we give AIRs and frame error rate (FER) results for our designed optimized concatenated codes for the memory- k nanopore channel model. We further compute AIRs and FER results for a real DNA channel using the experimental dataset in [6]. The dataset consists of 269709 output sequences taken from the output of an ONT MinION sequencer and also the corresponding input sequences (before synthesis). There are in total 10000 input sequences of length $N = 110$.

In all our simulations, we use $L_{\max} = 2$ and $d_{\max} = -d_{\min} = 5\sqrt{N \frac{\max(p_I, p_D)}{1 - \max(p_I, p_D)}}$, where p_I and p_D are the average insertion and deletion probabilities based on the dataset in [6]. Moreover, we use separate decoding as described in Section IV-B. The AIRs are computed by averaging over 10000 sequences of length $N = 110$.

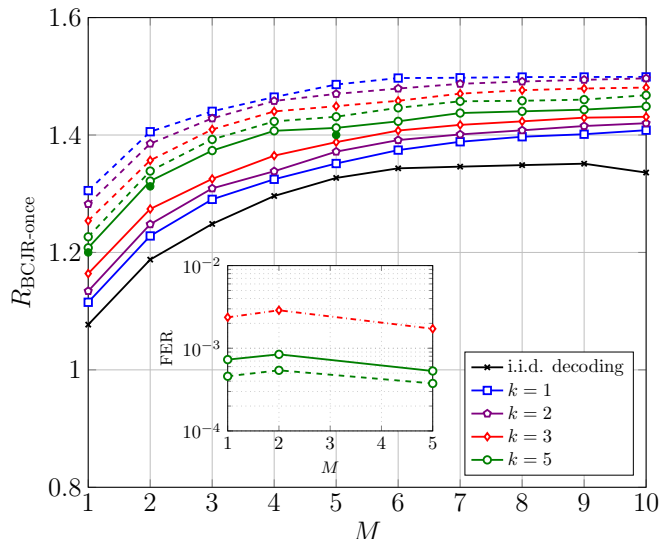


Fig. 3. BCJR-once rates with a rate- $3/2$ inner convolutional code for different values of M and $N = 110$. Solid curves are for the true channel and dashed curves for the memory- k nanopore channel model. The dash-dotted line is for decoding with $k = 3$ while the channel is set to $k = 5$. The green solid circles represent the rates for the outer LDPC codes with the optimized protographs in Table I.

In Fig. 3, we plot BCJR-once rates for the memory- k nanopore channel model (see Section II) with the convolutional code of Section VI-A as a synchronization inner code (dashed curves) for different values of k . For each k , the inner decoder is matched to the combination of the inner code and the memory- k nanopore channel model. Further, for each k , we estimated the transition probabilities of the memory- k nanopore channel model as described in Section II-A using the dataset in [6]. We observe that the AIRs decrease with increasing k . This is expected, as increasing the memory k makes the channel more complex.

In the figure, we also plot AIRs for the true DNA storage channel using the dataset in [6] (solid curves). (The random sequence added to the output of the inner code can be used to match the transmitted coded sequences to the input sequences of the dataset. Hence, the dataset can be used for the true channel with an inner convolutional code as well.) In this case, the curve for a given value of k corresponds to an AIR for the true DNA storage channel of a mismatched decoder where the inner decoder is matched to the combination of the inner code and the memory- k nanopore channel model. We observe the opposite effect to the AIRs for the memory- k nanopore channel, i.e., the AIRs increase with increasing k . Again, this behavior is expected: If the memory- k nanopore channel model models well the DNA storage channel (i.e., the assumption of a Markovian model is good), increasing k makes the decoder better matched to the true DNA storage channel, hence the AIR increases. Equivalently, a low value of k corresponds to a decoder that is more *mismatched* with respect to the true DNA storage channel, resulting in a lower AIR. Our results hence support that this channel model is good. In fact, although not directly apparent from the figure, the AIRs saturate when k increases, e.g., for the case of no

inner code (results not shown here) the AIRs saturate for k around 7. Furthermore, interestingly, comparing the dashed and solid curves, we observe a sandwich effect, where the AIR curve for the memory- k nanopore channel model (dashed curve with green circles) and the AIR for the true DNA storage channel with a mismatched decoder (matched to the combination of the inner code and the memory-5 nanopore channel model) are very close. This indicates that increasing k beyond 5 does not bring much further gains in AIR for the true DNA storage channel.

In Fig. 3, we also plot the BCJR-once rate for the true DNA storage channel of a decoder that assumes i.i.d. IDS errors (black curve with star markers), as most decoders in the literature. We observe that this results in a significant performance loss.

Finally, in the figure, we also plot the rate R obtained via DE for the true DNA storage channel for the outer LDPC codes with the optimized protographs in Table I (green filled circles), showing that our coding scheme gives excellent performance at code rates close to the BCJR-once rates.

In the inset of Fig. 3, we plot the FER results of our designed optimized concatenated codes with the inner convolutional code of Section VI-A and outer LDPC codes of length $N_o = 10000$ based on the protographs in Table I. The outer codeword is split into 123 subsequences of length 81, resulting in 110 channel input symbols after the inner encoding, and a single shorter subsequence of length 37. The codes are simulated over both the true DNA storage channel with an inner decoder matched to the memory-5 nanopore channel model (solid curve) and the memory-5 nanopore channel model for a decoder matched to $k = 5$ (green dashed curve with circles) and $k = 3$ (red dashed-dotted curve with diamonds). The results are in agreement with the DE results.

The decoding complexity increases exponentially with k (see Section IV-C). Thus, the AIRs and FER results in Fig. 3 allow us to quantify the performance loss incurred by a decoder assuming a given memory k and hence the trade-off between decoding complexity and error rate performance. We observe that considering memory 5 incurs almost no loss in terms of AIR, indicating that $k = 5$ is enough.

VIII. CONCLUSION

We derived the optimum MAP decoder for the memory- k nanopore channel model. Based on the MAP decoder, we derived AIRs for the true DNA storage channel of a mismatched decoder that is matched to the memory- k model and optimized coding schemes for this channel. We showed that, remarkably, the concatenated coding scheme in [4] (properly optimized) achieves excellent performance for the true DNA storage channel: Considering an optimal inner decoder for the memory- k nanopore channel yields significantly higher AIRs—hence higher storage density—for the true DNA storage channel than a decoder that assumes i.i.d. IDS errors, as usually assumed in the literature.

REFERENCES

- [1] G. M. Church, Y. Gao, and S. Kosuri, "Next-generation digital information storage in DNA," *Sci.*, vol. 337, no. 6102, p. 1628, Aug. 2012.
- [2] R. N. Grass, R. Heckel, M. Puddu, D. Paunescu, and W. J. Stark, "Robust chemical preservation of digital information on DNA in silica with error-correcting codes," *Angew. Chem. Int. Ed.*, vol. 54, no. 8, pp. 2552–2555, Feb. 2015.
- [3] S. M. H. T. Yazdi, R. Gabrys, and O. Milenkovic, "Portable and error-free DNA-based data storage," *Sci. Rep.*, vol. 7, no. 5011, pp. 1–6, Jul. 2017.
- [4] I. Maarouf, A. Lenz, L. Welter, A. Wachter-Zeh, E. Rosnes, and A. Graell i Amat, "Concatenated codes for multiple reads of a DNA sequence," *IEEE Trans. Inf. Theory*, vol. 69, no. 2, pp. 910–927, Feb. 2023.
- [5] I. Shomorony and R. Heckel, "Information-theoretic foundations of DNA data storage," *Found. Trends Commun. Inf. Theory*, vol. 19, no. 1, pp. 1–106, Feb. 2022.
- [6] S. R. Srinivasavaradhan, S. Gopi, H. D. Pfister, and S. Yekhanin, "Trellis BMA: Coded trace reconstruction on IDS channels for DNA storage," in *Proc. IEEE Int. Symp. Inf. Theory (ISIT)*, Melbourne, VIC, Australia, Jul. 2021, pp. 2453–2458.
- [7] M. C. Davey and D. J. C. MacKay, "Reliable communication over channels with insertions, deletions, and substitutions," *IEEE Trans. Inf. Theory*, vol. 47, no. 2, pp. 687–698, Feb. 2001.
- [8] J. A. Briffa, H. G. Schaathun, and S. Wesemeyer, "An improved decoding algorithm for the Davey-MacKay construction," in *Proc. IEEE Int. Conf. Commun. (ICC)*, Cape Town, South Africa, May 2010.
- [9] M. Inoue and H. Kaneko, "Adaptive synchronization marker for insertion/deletion/substitution error correction," in *Proc. IEEE Int. Symp. Inf. Theory (ISIT)*, Cambridge, MA, USA, Jul. 2012, pp. 508–512.
- [10] R. Shibata, G. Hosoya, and H. Yashima, "Design of irregular LDPC codes without markers for insertion/deletion channels," in *Proc. IEEE Glob. Commun. Conf. (GLOBECOM)*, Waikoloa, HI, USA, Dec. 2019.
- [11] H. Koremura and H. Kaneko, "Insertion/deletion/substitution error correction by a modified successive cancellation decoding of polar code," *IEICE Trans. Fundam. Electron., Commun. Comput. Sci.*, vol. E103.A, no. 4, pp. 695–703, Apr. 2020.
- [12] R. Sakogawa and H. Kaneko, "Symbolwise MAP estimation for multiple-trace insertion/deletion/substitution channels," in *Proc. IEEE Int. Symp. Inf. Theory (ISIT)*, Los Angeles, CA, USA, Jun. 2020, pp. 781–785.
- [13] R. Shibata, G. Hosoya, and H. Yashima, "Concatenated LDPC/trellis codes: Surpassing the symmetric information rate of channels with synchronization errors," *IEICE Trans. Fundam. Electron., Commun. Comput. Sci.*, vol. E103.A, no. 11, pp. 1283–1291, Nov. 2020.
- [14] H. D. Pfister and I. Tal, "Polar codes for channels with insertions, deletions, and substitutions," in *Proc. IEEE Int. Symp. Inf. Theory (ISIT)*, Melbourne, VIC, Australia, Jul. 2021, pp. 2554–2559.
- [15] M. F. Mansour and A. H. Tewfik, "Convolutional decoding in the presence of synchronization errors," *IEEE J. Sel. Areas Commun.*, vol. 28, no. 2, pp. 218–227, Feb. 2010.
- [16] V. Buttigieg and N. Farrugia, "Improved bit error rate performance of convolutional codes with synchronization errors," in *Proc. IEEE Int. Conf. Commun. (ICC)*, London, U.K., Jun. 2015, pp. 4077–4082.
- [17] B. Hamoum, E. Dupraz, L. Conde-Canencia, and D. Lavenier, "Channel model with memory for DNA data storage with nanopore sequencing," in *Proc. Int. Symp. Topics Coding (ISTC)*, Montréal, QC, Canada, Aug./Sep. 2021.
- [18] B. McBain, E. Viterbo, and J. Saunderson, "Finite-state semi-Markov channels for nanopore sequencing," in *Proc. IEEE Int. Symp. Inf. Theory (ISIT)*, Espoo, Finland, Jun./Jul. 2022, pp. 216–221.
- [19] L. R. Bahl and F. Jelinek, "Decoding for channels with insertions, deletions, and substitutions with applications to speech recognition," *IEEE Trans. Inf. Theory*, vol. 21, no. 4, pp. 404–411, Jul. 1975.
- [20] A. Kavčić, X. Ma, and M. Mitzenmacher, "Binary intersymbol interference channels: Gallager codes, density evolution, and code performance bounds," *IEEE Trans. Inf. Theory*, vol. 49, no. 7, pp. 1636–1652, Jul. 2003.
- [21] R. R. Müller and W. H. Gerstacker, "On the capacity loss due to separation of detection and decoding," *IEEE Trans. Inf. Theory*, vol. 50, no. 8, pp. 1769–1778, Aug. 2004.
- [22] J. B. Soriaga, H. D. Pfister, and P. H. Siegel, "Determining and approaching achievable rates of binary intersymbol interference channels using multistage decoding," *IEEE Trans. Inf. Theory*, vol. 53, no. 4, pp. 1416–1429, Apr. 2007.
- [23] X.-Y. Hu, E. Eleftheriou, and D.-M. Arnold, "Progressive edge-growth Tanner graphs," in *Proc. IEEE Glob. Telecommun. Conf. (GLOBECOM)*, San Antonio, TX, USA, Nov. 2001, pp. 995–1001.